Optimization of Cyclically Operated Reactors and Separators

T.L. van Noorden[1,2] S.M. Verduyn Lunel[3] A. Bliek[2] *

[1]Universiteit van Amsterdam, Department of Chemical Engineering, Nieuwe Achtergracht 166, 1018 WV Amsterdam, The Netherlands
[2]Vrije Universiteit Amsterdam, Department of Mathematics, De Boelelaan 1081A, 1081HV Amsterdam, The Netherlands,
[3]Universiteit Leiden, Department of Mathematics, Niels Bohrweg 1, 2333 CA Leiden, The Netherlands.

Abstract

An efficient numerical optimization procedure for the computation of solutions to periodic optimal control problems is presented. This procedure consists of a first order gradient method in combination with the Newton-Picard shooting method. The first order gradient method is able to compute the optimal control of a periodic process under one or more nonlocal constraints, such as a minimum purity constraint. The Newton-Picard method computes very efficiently periodic solutions to the state and adjoint equations. The presented numerical procedure is used to optimize a rapid pressure swing reactor and a rapid pressure swing adsorber. It is shown that the optimal cycle scheme consists of four steps: a no-inflow pre-pressurization step, a pressurization step, a no-inflow post-pressurization step, and a depressurization step.

Keywords: Optimisation, Cyclic processes, Process control, Packed bed, Numerical analysis, Dynamic simulation

1 Introduction

This paper is devoted to the numerical optimization of periodic adsorbers and reactors. Periodic adsorbers and reactors are processes with periodically changing control parameters and boundary conditions. Examples are pressure swing adsorption processes, where

*Corresponding author. e-mail: bliek@science.uva.nl

the pressure changes periodically, temperature swing adsorption processes, where the temperature changes periodically and the reverse flow reactor, where the flow direction changes periodically. Periodic adsorbers and reactors are intrinsically dynamic processes, operated in a cyclic mode with a fixed cycle time. After a number of start up cycles, such a cyclic process will usually approach a periodic state, that is, a limiting state, in which the conditions in the bed at the end of each cycle are identical to those at its start.

The performance of a periodic adsorber or reactor is critically affected by a large number of design and operating parameters. These include, for example, the size of the bed(s), the physical characteristics of the adsorbent and the catalyst, the duration of the various steps in the cycle and the pressure levels in each step. Due to the large number of variables and parameters, the numerical optimization of a periodic process can be a computationally very expensive task.

We would like to make the following distinction between two different kinds of optimization: the optimization with respect to time-independent parameters and the optimization with respect to time-dependent parameters, also known as optimal control. In this paper we would like to focus on the numerical optimal control of periodic processes, although we also optimize the presented example systems with respect to time-independent parameters. The reason for this is that for time-independent parameter optimization a large number of different methods and algorithms are readily available in many software packages and libraries, whereas the time-dependent parameter optimization, or optimal control, of periodic systems is much less a standard task.

The numerical optimization of a periodic process is typically aiming to minimize operating costs, or to maximize product yield, while maintaining certain product specifications, such as a minimum purity. In this paper an efficient numerical optimization procedure for the computation of solutions to periodic optimal control problems is presented. The procedure is able to compute the optimal control of a periodic process under one or more nonlocal constraints, such as the minimum purity constraint. The presented method consists of a combination of the Newton-Picard shooting method (Van Noorden et al., 2002, 2001; Lust et al., 1998) with a first order gradient method (Bryson Jr. and Ho, 1975).

Basically, we are using the same technique as used by Horn and Lin (1967) and Kowler and Kadlec (1972); these authors use a combination of a first order gradient method with Newton's method. Due to the rapid increase in computational effort as the dimension of the system grows, in these two papers, this technique was only applied to low dimensional systems. The interaction with the Newton-Picard method makes the first order gradient method much more efficient. Therefore we can apply the first order gradient method to higher dimensional systems and thus we are able to make much more accurate computations.

Other work on the optimization of periodic processes can be found in (Kvamsdal and Hertzberg, 1997), where a trace separation system is optimized. In (Kvamsdal and Hertzberg, 1995), the same authors consider the efficient determination of periodic states of cyclic processes. In (Nilchan and Pantelides, 1998) a complete discretization approach is used to determine periodic states and optimize two periodic adsorption processes. Stepanek et al. (1998) employ quasi-Newton methods for the efficient optimization of a continuous adsorption process in a dessicant rotor.

We use the in this paper presented numerical method to optimize a rapid pressure swing adsorber (Nilchan and Pantelides, 1998) and a rapid pressure swing reactor (Cheng et al., 1998). We also show that the results of these two time-dependent parameter optimization problems can help to gain insight in the solution of a time-independent parameter optimization problem. For the computation of the solution to the time-independent parameter optimization problems we use a sequential quadratic programming method (NAG fortran library routine E04UCF)

The organization of this paper is as follows. In Section 2 we discuss the model equations of a rapid pressure swing adsorber (Nilchan and Pantelides, 1998) and of a rapid pressure swing reactor (Cheng et al., 1998) and give the results of the optimization of these two systems. In Section 3 we present the numerical method, which consists of the combination of a first order gradient method with the Newton-Picard method, used to obtain the results in Section 2. In Section 3 we also discuss the efficiency of this combination of methods.

2 The Optimization of Two Rapid Pressure Swing Processes

In this section we will present the model equations and discuss the optimization of a rapid pressure swing adsorber and of a rapid pressure swing reactor.

2.1 The Rapid Pressure Swing Adsorber

2.1.1 The Model Equations

Pressure swing adsorption processes are systems that separate mixtures of gases by periodically varying the pressure over an adsorption bed. Among the pressure swing adsorption processes, the Rapid Pressure Swing Adsorption process (RPSA) offers one of the simplest configurations. The RPSA cycle comprises two basic steps: pressurization by feed gas and counter-current depressurization with internal purging. Both steps have a short time duration, in the order of several seconds. The adsorption bed consists of small adsorbent particles with average size between 200-700 μm. The effectiveness of self purging within the RPSA bed results from a combination of a fast cycle time together with a small particle size leading to steep and periodically varying pressure gradients within the bed. The pressure at the product end is approximately constant over time and this renders continuous product release possible.

The specific application of interest to this case study is air purification using an adsorption bed of zeolite A5 which preferentially adsorbs nitrogen and leaves oxygen in the product stream. The model is taken from Nilchan and Pantelides (1998).

The model gas consists of two components, oxygen and nitrogen. The variables in the model are the gas phase concentrations of these two components, denoted by $c^{(i)} = c^{(i)}(t,z)$, $0 \le t < \infty$ and $0 \le z \le 1$, ($i=1$: oxygen, $i=2$: nitrogen), the adsorbed amount of the two components, denoted by $q^{(i)} = q^{(i)}(t,z)$, $0 \le z < \infty$ and $0 \le t \le 1$, and the gas phase velocity $v = v(t,z)$, $0 \le t < \infty$ and $0 \le z \le 1$. Note that the dimensionless cycle time is rescaled to become one time unit. This means the physical cycle time appears as a parameter in the model equations and is denote by T. The model equations consist of the gas phase balance equations

$$c_t^{(i)} = TC_1 c_{zz}^{(i)} - C_2 (vc^{(i)})_z - C_3^{(i)} q_t^{(i)}, \quad i = 1,2, \tag{1}$$

the adsorption rate equations

$$q_t^{(i)} = \frac{Tk^{(i)}}{c^{(1)} + c^{(2)} + D^{(i)}} (c^{(i)} - q^{(i)}), \quad i = 1,2, \tag{2}$$

and the gas phase velocity equation

$$v(t,z) = -TC_4 \big(c_z^{(1)}(t,z) + c_z^{(2)}(t,z)\big). \tag{3}$$

Note that the equations are autonomous, but the boundary conditions are periodic in time. In fact, at the feed end (at $z=0$) of the adsorber there are two sets of alternating boundary conditions. During the first step, the so-called *pressurization step*, the boundary conditions are

$$\begin{cases} TC_1 c_z^{(i)}(t,0) = C_2 v(t,0)(c^{(i)}(t,0) - y_f^{(i)} p_f), \quad i = 1,2 \\ c^{(1)}(t,0) + c^{(2)}(t,0) = p_f \end{cases} \quad \text{for } 0 \le t \,(\text{mod } 1) < t_f. \tag{4}$$

During the second step, the so-called *depressurization step*, the boundary conditions are

$$\begin{cases} c_z^{(i)}(t,0) = 0, \quad i = 1,2 \\ c^{(1)}(t,0) + c^{(2)}(t,0) = p_w \end{cases} \quad \text{for } t_f \le t \,(\text{mod } 1) \le 1. \tag{5}$$

The boundary conditions at the product end (at $z=1$) of the adsorber are given by

$$\begin{cases} c_z^{(i)}(t,1) = 0, \quad i = 1,2 \\ v(t,1) = TC_5 \big(c^{(1)}(t,1) + c^{(2)}(t,1)\big)^{-1} \end{cases} \tag{6}$$

Table 1: The dimensionless parameter values for the RPSA process. The superscripts (1) and (2) denote respectively component 1 (oxigen) and component 2 (nitrogen). The physical parameter values can be found in (Nilchan and Pantelides, 1998).

C_1	0.0014	C_2	1.4134
$C_3^{(1)}$	3.8988	$C_3^{(2)}$	8.3975
C_4	0.616	C_5	0.0024
$k^{(1)}$	146.07	$k^{(2)}$	67.82
$D^{(1)}$	0.5351	$D^{(2)}$	0.5007
$y_f^{(1)}$	0.21	$y_f^{(2)}$	0.79
p_w	0.4717	t_f	0.5
a	1.24	b	1.4

The equations (1)-(3) together with the boundary conditions (4)-(6) complete the description of the RPSA model. A solution of (1)-(3) together with the boundary conditions (4)-(6) that satisfies

$$\begin{cases} c^{(i)}(0,\cdot) = c^{(i)}(1,\cdot), \\ q^{(i)}(0,\cdot) = q^{(i)}(1,\cdot), \end{cases} \quad i = 1, 2,$$

is called a periodic solution of the RPSA model.

The dimensionless parameters that appear in the equations are denoted by T, C_1, C_2, $C_3^{(i)}$, C_4, C_5, $k^{(i)}$, $D^{(i)}$, $y_f^{(i)}$, p_w, p_f and t_f. The parameters T (cycle time), p_f (feed pressure) and t_f (ratio between the two step lengths) are used to optimize the process. The values of the other parameters are listed in Table 1.

2.1.2 The Performance Index and the Constraints

For the optimization of the RPSA process we will use a measure for the performance of the process, the so-called performance index. For the PRSA process, we would like to minimize the average power requirements of the compressor during the pressurization step. Thus the performance index to be minimized, is the average power, which is given by

$$V = \frac{P_0}{T} \int_0^{t_f} v(t,0) p_f (a(p_f)^{(b-1)/b} - 1) dt,$$

where P_0 is the characteristic power (for the values of the parameters as given in Table 1 we obtain P_0=184.53 [W=J/s]). We wish to optimize this performance index with the constraint that the purity of the product gas is at least 87 %. This purity is given by

$$Pu = \int_0^1 \frac{c^{(1)}(t,1)}{c^{(1)}(t,1) + c^{(2)}(t,1)} dt.$$

2.1.3 Optimization Results

The model equations are discretized on 20 nodes using a second order finite volumes approximation. For the time integration of the resulting system of 80 ($N = 80$) ordinary differential equations, the fortran NAG library routine D02EJF is used.

The first step is to optimize the RPSA with respect to the feed pressure p_f, the duration of the pressurization step t_f, and the duration of the cycle T. The reference case values are given by

$$p_f = 1, \quad t_1 = 0.5, \quad \text{and } T = 3.$$

For these values a purity level of 87.2 % is obtained and the value of the performance index equals 109.4.

For the optimization with respect to these parameters we use the fortran NAG library routine E04UCF (a sequential quadratic programming method). This routine gives the following values for the optimal parameters

$$p_f = 0.998, \quad t_f = 0.201, \quad \text{and } T = 8.38. \tag{7}$$

For these values a purity level of 87.0 % is obtained and the corresponding value of the performance index equals 53.9. This is a reduction of more than 50 % with respect to the reference case values.

Since the performance index depends strongly on the feed pressure, the performance index is expected to decrease even further when compared to the three parameter optimization, when the feed pressure is allowed to vary continuously in time.

For the computation of the optimal feed pressure history, we fix the cycle duration T to be equal to 8 and the (dimensionless) duration of the pressurization step to be equal to 0.5. Note that the boundary condition (4) needs careful attention. Indeed, the feed pressure may not become so low that the gas velocity at the feed end of the adsorber becomes negative. Therefore, it is more convenient to choose the gas velocity at the entrance of the adsorber as the control parameter instead of the feed pressure. Once the periodic state has been computed, the optimal gas velocity history can be used to obtain the optimal feed pressure history without affecting the periodic state.

The resulting optimal gas velocity and feed pressure histories are given in Fig. 1. For this feed pressure history, the purity turns out to be 87.0 % and the performance index is 36.87. This is a considerable improvement compared to the solution of the minimization using only constant parameters.

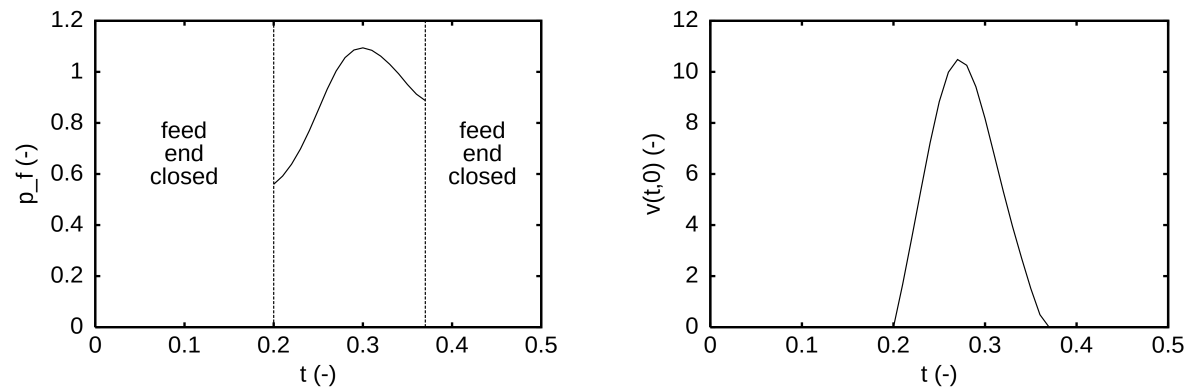

Figure 1: The dimensionless feed pressure p_f (left figure) and the dimensionless feed velocity $v(t, 0)$ (right figure) versus the dimensionless time t for the optimal time-programmed feed velocity for the RPSA with parameter values as in Table 1. A purity of 87.0 % is obtained and the performance index equals 36.87

From the graph of the gas velocity history in Fig. 1, it is seen that at the beginning and at the end of the pressurization step, the gas velocity is equal to zero for some time. This situation can also be accomplished by closing the feed end of the adsorber. This suggests that, even when it is not possible to control the feed pressure continuously, the performance index can still be decreased by incorporating two more steps in the cycle scheme. This cycle scheme can be described by the following sets of boundary conditions. During the first step, *the pre-pressurization step*, the boundary conditions are

$$\begin{cases} c_z^{(i)}(t,0) = 0, \quad i = 1,2 \\ v(t,0) = 0 \end{cases} \quad \text{for } 0 \le t \,(\mathrm{mod}\ 1) < t_1.$$

During the second step, *the pressurization step*, the boundary conditions are

$$\begin{cases} TC_1 c_z^{(i)}(t,0) = C_2 v(t,0)(c^{(i)}(t,0) - y_f^{(i)} p_f), \quad i = 1,2 \\ c^{(1)}(t,0) + c^{(2)}(t,0) = p_f \end{cases} \quad \text{for } t_1 \le t \,(\mathrm{mod}\ 1) < t_1 + t_2.$$

During the third step, *the post-pressurization step*, the boundary conditions are the same as in the first step:

$$\begin{cases} c_z^{(i)}(t,0) = 0, \quad i = 1,2 \\ v(t,0) = 0 \end{cases} \quad \text{for } t_1 + t_2 \le t \,(\mathrm{mod}\ 1) < t_1 + t_2 + t_3.$$

During the fourth step, *the depressurization step*, the boundary conditions are

$$\begin{cases} c_z^{(i)}(t,0) = 0, \quad i = 1,2 \\ c^{(1)}(t,0) + c^{(2)}(t,0) = p_w \end{cases} \quad \text{for } t_1 + t_2 + t_3 \le t \,(\mathrm{mod}\ 1) \le 1.$$

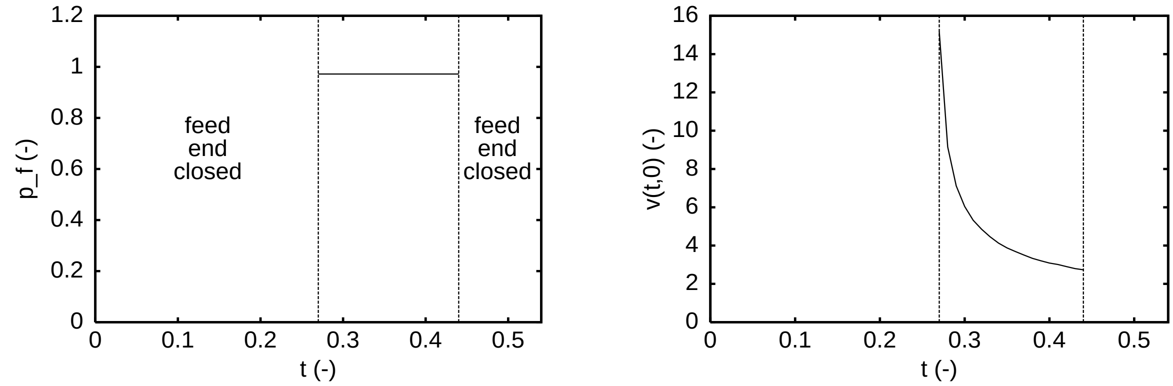

Figure 2: The dimensionless feed pressure p_f (left figure) and the dimensionless feed velocity $v(t, 0)$ (right figure) versus the dimensionless time t for the optimal four step cycle for the RPSA with parameter values as in Table 1. A purity of 87.0 % is obtained and the performance index equals 41.0.

Note that in this step the boundary conditions are again the same as for the original depressurization step.

If we now minimize the performance index with respect to the parameters t_1, t_2, t_3, t_4, p_f and T, again using the fortran NAG library routine E04UCF, the following values are obtained

$$t_1 = 0.263, \quad t_2 = 0.179, \quad t_3 = 0.097, \quad T = 7.73, \quad \text{and } p_f = 0.972.$$

The corresponding purity is 87.0% and the value of the performance index equals 41.0. This is approximately a 25% improvement compared to the three parameter minimization (7). The corresponding cycle scheme is depicted in Fig. 2.

2.2 The Rapid Pressure Swing Reactor

2.2.1 The Model Equations

This second system under consideration consists of a single bed, which is packed with a mixture of an active catalyst for the reaction, and a selective adsorbent for the adsorption of one or more of the reaction species. The process is operated with two basic steps: feed gas pressurization and counter-current depressurization. In the pressurization step, feed is introduced at a pressure higher than atmospheric pressure. Adsorption and reaction occur simultaneously within the reactor. Different component adsorption capacities promote separation of the reactants from the products and thus may increase conversion of the reactant and/or selectivity of the desired product. In the depressurization step, the pressure in the bed is reduced to atmospheric pressure, the adsorbed species are desorbed and the bed is subsequently regenerated. Both steps have a short time duration, in the order of several seconds. The adsorption bed consists of small adsorbent particles with average size between 200-700 μm. This combination of a fast cycle time together with a small particle size leads to steep and periodically varying pressure gradients within the bed. The pressure at the product end is approximately constant over time and this makes the process useful for continuous product release.

A reversible dissociation reaction, 2A $\rightleftharpoons$ B + C, is investigated. The model is taken from Cheng et al. (1998). The model gas consists of three components, A, B and C. The variables in the model are the gas phase concentrations of these three components, denoted by $c^{(i)} = c^{(i)}(t,z)$, $0 \le t < \infty$ and $0 \le z \le 1$ (with $i=1$: A, $i=2$: B and $i=3$: C), the adsorbed amount of the three components, denoted by $q^{(i)} = q^{(i)}(t,z)$, $0 \le t < \infty$ and $0 \le z \le 1$, and the gas phase velocity $v = v(t,z)$, $0 \le t < \infty$ and $0 \le z \le 1$. Note that the dimensionless cycle time is rescaled to become one time unit. This means the physical cycle time appears as a parameter in the model equations and is denote by T. The model equations consist of the gas phase balance equations

$$c_t^{(i)} = TC_1 c_{zz}^{(i)} - C_2(vc^{(i)})_z - C_3^{(i)} q_t^{(i)} - Tk^{(i)} r(c^{(1)}, c^{(2)}, c^{(3)}), \quad i = 1,2,3, \tag{8}$$

the adsorption rate equations

$$q_t^{(i)} = c_t^{(i)}, \quad i = 1,2,3, \tag{9}$$

the gas phase velocity equation

$$v(t,z) = -TC_4\big(c_z^{(1)}(t,z) + c_z^{(2)}(t,z) + c_z^{(3)}(t,z)\big), \tag{10}$$

and the reaction rate equation

$$r\big(c^{(1)}(t,z), c^{(2)}(t,z), c^{(3)}(t,z)\big) = \left(c^{(1)}(t,z)^2 - \frac{c^{(2)}(t,z)c^{(3)}(t,z)}{K}\right). \tag{11}$$

Note that the equations are autonomous, but that the boundary conditions are periodic in time. In fact, at the feed end (at $z = 0$) of the reactor there are two sets of alternating boundary conditions. During the first step, the so-called *pressurization step*, the boundary conditions are

$$\begin{cases} TC_1 c_z^{(i)}(t,0) = C_2 v(t,0)(c^{(i)}(t,0) - y_f^{(i)} p_f), \quad i = 1,2,3 \\ c^{(1)}(t,0) + c^{(2)}(t,0) + c^{(3)}(t,0) = p_f \end{cases} \text{for } 0 \le t \,(\mathrm{mod}\ 1) < t_f. \tag{12}$$

During the second step, the so-called *depressurization step*, the boundary conditions are

$$\begin{cases} c_z^{(i)}(t,0) = 0, \quad i = 1,2,3 \\ c^{(1)}(t,0) + c^{(2)}(t,0) + c^{(3)}(t,0) = p_w \end{cases} \text{for } t_f \le t \,(\mathrm{mod}\ 1) \le 1. \tag{13}$$

Table 2: The dimensionless parameter values for the RPSR process. The superscripts (1), (2) and (3) denote respectively component A, B and C. The physical parameter values can be found in (Cheng et al., 1998).

C_1	$1.40{\cdot}10^{-5}$	C_2	1.40
$C_3^{(1)}$	0	$C_3^{(2)}$	0
$C_3^{(3)}$	1.163	C_4	1.064
C_5	0.000170	$k^{(1)}$	36198
$k^{(2)}$	-18099	$k^{(3)}$	-18099
K	0.0156	$y_f^{(1)}$	1
$y_f^{(2)}$	0	$y_f^{(3)}$	0
p_f	1	p_w	0.33
t_f	0.5		

The boundary conditions at the product end (at $z = 1$) of the reactor are given by

$$\begin{cases} c_z^{(i)}(t,1) = 0, \quad i = 1,2,3 \\ v(t,1) = TC_5\big(c^{(1)}(t,1) + c^{(2)}(t,1) + c^{(3)}(t,1)\big)^{-1} \end{cases} \tag{14}$$

The equations (8)-(11) together with the boundary conditions (12)-(14) complete the description of the RPSR model. A solution of (8)-(11) together with the boundary conditions (12)-(14) that satisfies

$$\begin{cases} c^{(i)}(0,\cdot) = c^{(i)}(1,\cdot), \\ q^{(i)}(0,\cdot) = q^{(i)}(1,\cdot), \end{cases} \quad i = 1,2,3$$

is called a periodic solution of the RPSR model. The dimensionless parameters that appear in the equations are denoted by T, C_1, C_2, $C_3^{(i)}$, C_4, C_5, $k^{(i)}$, $m^{(i)}$, $y_f^{(i)}$, K, p_w, p_f and t_f. The parameters T (cycle time), p_f (feed pressure) and t_f (ratio between the two step lengths) are used to optimize the process. The values of the other parameters are listed in Table 2.

2.2.2 The Performance Index and the Constraints

Also for the optimization of the RPSR process we need a measure for the performance of the process. For the PRSR process, we would like to optimize the yield of the pure product B. Thus the performance index to be maximized, is the yield of the component B, which is given by

$$Y = \frac{\displaystyle\int_0^1 v(t,1)c^{(2)}(t,1)dt}{\displaystyle\int_0^{t_f} v(t,0)c^{(1)}(t,0)dt}.$$

We wish to optimize this performance index with the constraint that the purity of the product gas is at least 95 %. The purity of the product gas is given by

$$Pu = \int_0^1 \frac{c^{(2)}(t,1)}{c^{(1)}(t,1) + c^{(2)}(t,1) + c^{(3)}(t,1)} dt.$$

2.2.3 Optimization Results

We discretize the model equations on 20 nodes using a third order upwind finite volumes approximation. For the time integration of the resulting system of 60 ($N = 60$) ordinary differential equations, the fortran NAG library routine D02EJF is used. Here we take as control parameters the feed pressure p_f, the duration of the pressurization step t_f, and the duration of the cycle T. The reference case values are given by

$$p_f = 1, \quad t_1 = 0.5, \quad \text{and } T = 4.5.$$

For these values a purity level of 92.31 % is obtained and the corresponding value of the performance index equals 0.0014. Note that these parameters do not satisfy the constraint on the purity.

We use the fortran NAG library routine E04UCF (a sequential quadratic programming method) to find the optimal values of the parameters that do satisfy the purity constraint. This routine gives the following values for the optimal parameters

$$p_f = 1.12474, \quad t_f = 0.431, \quad \text{and } T = 4.46567.$$

For these values a purity level of 94.9922 % is obtained and value of the performance index equals 0.0012.

It is expected that, when the feed pressure is allowed to vary continuously in time, the performance index can be increased even further in comparison with the previous three parameter optimization.

For the computation of the optimal feed pressure history, we fix the cycle duration T to 4.41 and the (dimensionless) duration of the pressurization step to 0.5. We again have to pay attention to the boundary condition (12). For the same reason as for the RPSA process, also for the RPSR the gas velocity at the entrance of the reactor is used as the control parameter, rather than the feed pressure.

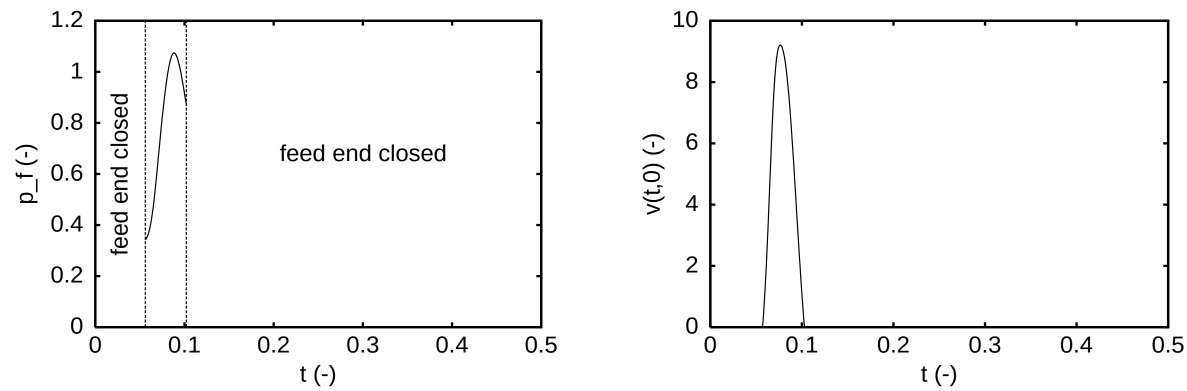

Figure 3: The dimensionless feed pressure p_f (left figure) and the dimensionless feed velocity $v(t,0)$ (right figure) versus the dimensionless time t for the optimal time-programmed feed velocity for the RPSR with parameter values as in Table 2. A purity of 95.0 % is obtained and the performance index equals 0.00339.

The resulting optimal gas velocity and feed pressure histories are given in Fig. 3. For this feed pressure history, the purity turns out to be 95.0 % and the performance index is 0.00339. This is a considerable improvement compared to the solution of the optimization using only time-independent parameters.

From the graph of the gas velocity history in Fig. 3 it is seen that at the beginning and at the end of the pressurization step the gas velocity is equal to zero for some time. This means that also for the RPSR, the performance index may still be decreased by incorporating two more steps in the cycle scheme. This four-step cycle scheme can be described by the following sets of boundary conditions. During the first step, *the pre-pressurization step*, the boundary conditions are

$$\begin{cases} c_z^{(i)}(t,0) = 0, \quad i = 1,2,3 \\ v(t,0) = 0 \end{cases} \quad \text{for } 0 \leq t \,(\text{mod } 1) < t_1.$$

During the second step, *the pressurization step*, the boundary conditions are

$$\begin{cases} TC_1 c_z^{(i)}(t,0) = C_2 v(t,0)(c^{(i)}(t,0) - y_f^{(i)} p_f), \quad i = 1,2,3 \\ c^{(1)}(t,0) + c^{(2)}(t,0) + c^{(3)}(t,0) = p_f \end{cases} \quad \text{for } t_1 \leq t \,(\text{mod } 1) < t_1 + t_2.$$

During the third step, *the post-pressurization step*, the boundary conditions are the same as in the first step:

$$\begin{cases} c_z^{(i)}(t,0) = 0, \quad i = 1,2,3 \\ v(t,0) = 0 \end{cases} \quad \text{for } t_1 + t_2 \leq t \,(\text{mod } 1) < t_1 + t_2 + t_3.$$

During the fourth step, *the depressurization step*, the boundary conditions are

$$\begin{cases} c_z^{(i)}(t,0) = 0, \quad i = 1,2,3 \\ c^{(1)}(t,0) + c^{(2)}(t,0) + c^{(3)}(t,0) = p_w \end{cases} \quad \text{for } t_1 + t_2 + t_3 \leq t \,(\text{mod } 1) \leq 1.$$

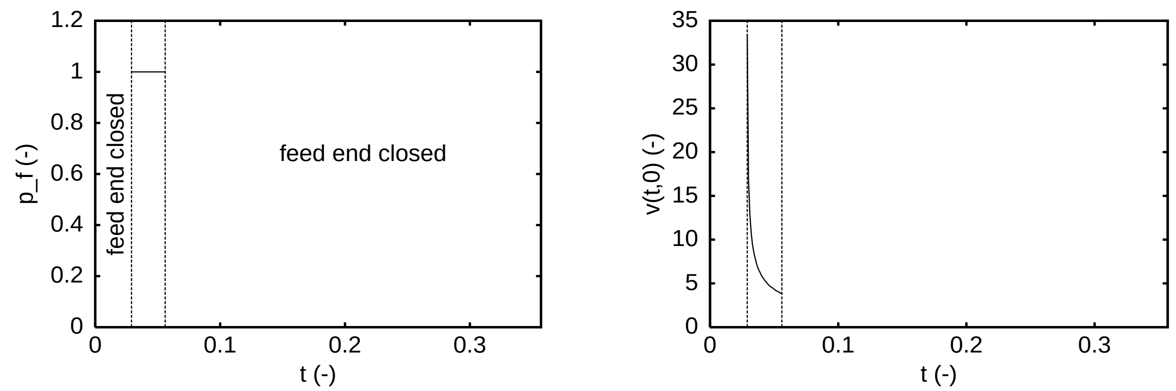

Figure 4: The dimensionless feed pressure p_f (left figure) and the dimensionless feed velocity $v(t,0)$ (right figure) versus the dimensionless time t for the optimal four step cycle for the RPSR with parameter values as in Table 2. A purity of 95.06 % is obtained and the performance index equals 000338.

Note that in this step the boundary conditions are again the same as for the original depressurization step.

If we now optimize the performance index with respect to the parameters t_1, t_2, t_3, t_4, p_f and T, again using the fortran NAG library routine E04UCF, the following values are obtained

$$t_1 = 0.0286, \quad t_2 = 0.0282, \quad t_3 = 0.301, \quad T = 4.485, \quad \text{and } p_f = 1.000.$$

The corresponding purity is 95.06% and the value of the performance index equals 0.00338. This optimum is very close to the optimal control and it improves the performance index by approximately 300% compared to the three parameter optimization (15). The corresponding cycle scheme is depicted in Fig. 4

Thus we see that, for both the RPSA and the RPSR, even in the case it is not possible to vary the control parameter continuously in time, it is fruitful to consider the solution to the optimal control problem. From this solution, insight can be obtained on how to change the cycle scheme in order to improve the performance of the process. In case of the studied rapid pressure swing processes, it is observed that the incorporation of two additional steps in the cycle scheme greatly improves the performance of the process using only time-independent control parameters. We therefore believe that the numerical procedure to compute solutions to the optimal control problem, that we have used to obtain the results in this section and that we present in the next section, can be an important tool in the study of periodic processes.

3 Numerical Periodic Optimal Control

In this section we will start with an introduction to the mathematical formulation of the optimal control problem. We will formulate the first order gradient algorithm following the work by Bryson Jr. and Ho (1975).

Subsequently the efficient interaction between the first oder gradient method and the Newton-Picard method is discussed in detail. This concerns in particular the steps of the gradient method in which the Newton-Picard method is used to compute periodic solutions to the state and adjoint equations.

3.1 Problem Formulation

The common approach to model a pressure swing adsorber or reactor leads to a system of partial differential equations with periodic boundary conditions. In order to investigate the behaviour of the solutions to this system of partial differential equations numerically, the system has to be discretized in space. This leads to a large system of N (where N depends on the space discretization) time periodic ordinary differential equations. This system can be written as

$$\dot{x}(t) = F(t, x(t), u(t)) \ , \ \ \text{where} \ \ F(t+1, \cdot, u(t+1)) = F(t, \cdot, u(t)) \ , \tag{15}$$

where $x(t)$ is a N dimensional vector, $u(t)$ is a scalar 1-periodic control, and where $F(t, \cdot, u(t))$ is a function from the N dimensional vectors (denoted by $\mathbb{R}^N$) to the N dimensional vectors.

Since for optimization purposes we are only interested in periodic states of the system, we can restrict ourselves to consider solutions of (15) for $t \in [0, 1]$, supplemented with the periodic boundary conditions

$$x(0) = x(1). \tag{16}$$

The values that $u(t)$ can attain are restricted to a given interval B, say $B := [\alpha, \beta]$, i.e.,

$$\alpha \leq u(t) \leq \beta \text{ for all } t \in [0, 1]. \tag{17}$$

Furthermore, given the functionals L and M, depending on time, the state variables and the control parameter, we define the performance index

$$I(x, u) = \int_0^1 L(t, x(t), u(t))\, dt, \tag{18}$$

and a non-local constraint

$$\tilde{I}(x, u) = \int_0^1 M(t, x(t), u(t))\, dt = 0, \tag{19}$$

The optimal control problem, denoted by (OPC), now consists of finding a control $u(t)$ that minimize the performance index (18) under the constraints (15), (16), (17) and (19).

3.2 A First Order Gradient Method

In this section we describe the basic steps of the numerical procedure that we have implemented. We start with an overview of the procedure and then in the next section we concentrate on the steps 2 and 3 since in these two steps we use the Newton-Picard method as a new approach to make the first order gradient method more efficient.

Optimal Control Algorithm

Step 1: *Choose an initial control $u_0(t)$ and two positive scalars ϵ_1 and ϵ_2. Set $v(t) = u_0(t)$.*

Step 2: *Compute the periodic solution $x(t)$ of*

$$\dot{x}(t) = F(t, x(t), v(t)), \quad x(0) = x(1).$$

Step 3 *Compute solutions $\Lambda(t)$ and $R(t)$ of*

$$\frac{d}{dt}\Lambda^T(t) = -\Lambda^T(t)\frac{\partial F}{\partial x}(t, x(t), v(t)) - \frac{\partial L}{\partial x}(t, x(t), v(t)), \tag{20}$$

$$\frac{d}{dt}R^T(t) = -R^T(t)\frac{\partial F}{\partial x}(t, x(t), v(t)) - \frac{\partial M}{\partial x}(t, x(t), v(t)), \tag{21}$$

with the periodic boundary conditions $\Lambda(0) = \Lambda(1)$ and $R(0) = R(1)$.

Step 4: *Compute the integrals*

$$I_1 = \int_\Omega \left[R^T\frac{\partial F}{\partial u} + \frac{\partial M}{\partial u}\right]\left[R^T\frac{\partial F}{\partial u} + \frac{\partial M}{\partial u}\right]^T dt,$$

$$I_2 = \int_\Omega \left[\Lambda^T\frac{\partial F}{\partial u} + \frac{\partial L}{\partial u}\right]\left[R^T\frac{\partial F}{\partial u} + \frac{\partial M}{\partial u}\right]^T dt,$$

$$I_3 = \int_\Omega \left[\Lambda^T\frac{\partial F}{\partial u} + \frac{\partial L}{\partial u}\right]\left[\Lambda^T\frac{\partial F}{\partial u} + \frac{\partial L}{\partial u}\right]^T dt,$$

where $\Omega \subseteq [0,1]$ with $\Omega = \{t \in [0,1] \mid a < u_0(t) < b\}$.

Step 5: *Compute Δu*

$$\Delta u(t) = -\epsilon_2\Big[\frac{\partial L}{\partial u}(t, x(t), v(t)) + \nu\frac{\partial M}{\partial u}(t, x(t), v(t)) \\ + [\Lambda(t) + R(t)\nu]^T\frac{\partial F}{\partial u}(t, x(t), v(t))\Big],$$

with

$$\nu = (\epsilon_2 I_1)^{-1}(\epsilon_1 \int_0^1 M(t, x(t), v(t))\, dt - \epsilon_2 I_2).$$

Set $u(t) = v(t) + \Delta u(t)$ *and define the new control* $v(t) = u(t) + \max(a - u(t), 0) - \max(u(t) - b, 0)$. *This is done to make sure that the new control is in* $[a, b]$. *Go to* **Step 2**.

Note that the performance of the algorithm depends on the so-called damping factors ϵ_1 and ϵ_2. If the algorithm does not converge, then ϵ_1 and ϵ_2 should be chosen smaller. If the algorithm converges very slowly then ϵ_1 and ϵ_2 should be chosen larger, see (Bryson Jr. and Ho, 1975).

3.3 Computing Periodic Solutions of the State and Adjoint Equations

In Step 2 and Step 3 of the algorithm introduced in the Section 3.2 we have to find a periodic solution $x(t)$ of the state equation (15) and periodic solutions $\Lambda(t)$ and $(R(t)$ of the adjoint equations (20) and (21). In this section we discuss the Newton-Picard method that can be used to compute such periodic solutions.

The efficiency of the combination of the first order gradient method with the Newton-Picard method, lies in the fact that the Newton-Picard method does not only compute a periodic solution of the state equations (15), but also obtains information about the stability of this periodic solution. This information is used to compute very efficiently solutions to the adjoint equations (20) and (21).

First, solutions of (15) are discussed. In order to describe the Newton-Picard method, we introduce the map $G_u : \mathbb{R}^N \to \mathbb{R}^N$ that for a given control $u(t)$ assigns to the initial data at time zero, $x(0) = x_0$, the value of the solution of (15) after one cycle, i.e.,

$$G_u(x_0) = x(1, x_0),$$

where $x(t, x_0)$ is the solution of equation (15) with initial condition $x(0) = x_0$. This map is called the Poincaré or period map of (15). Note that evaluating the map G_u at x_0 is equivalent to simulating *one* cycle of the process for the control $u(t)$, starting with a given initial condition x_0.

A periodic state of the chemical system is a 1-periodic solution $x(t, x_0)$, i.e., a solution with $x(1, x_0) = x_0$, of (15), and thus the initial condition of a periodic solution is a fixed point of the equation $x = G_u(x)$. The Newton-Picard method is a new, recently developed method to compute solutions to this fixed point equation.

The philosophy underlying the Newton-Picard method (Lust et al., 1998) is to combine the favourable properties of both Newton's method and of dynamic simulation. Newton's method converges quadratically, but each iteration requires a large computational effort in terms of the number of cycles simulated. On the other hand, the dynamic simulation converges often very slowly, using many cycle iterations. In order to combine the strategies of both methods, we divide the state space into a part in which the dynamic simulation converges quickly and a part in which it is more efficient to use Newton's method.

The Newton-Picard method is a quasi-Newton method. This means that the method produces approximations to a fixed point of G_u, using the iteration scheme

$$\begin{cases} x_{i+1} = x_i + \Delta x_i \text{ with} \\ \Delta x_i \approx -(J(x_i) - I)^{-1}(G_u(x_i) - x_i), \end{cases} \tag{22}$$

where $J(x_i)$ denotes the Jacobian of G_u at x_i.

Fix i, set $x = x_i$ and assume that the eigenvalues μ_1, μ_2, ..., μ_N of $J(x)$ are known, ordered by decreasing modulus

$$|\mu_1| \geq |\mu_2| \geq ... \geq |\mu_p| > \rho > |\mu_{p+1}| \geq ... \geq |\mu_N|,$$

where ρ is a free parameter of the method. Define U to be the subspace of the discretized state space $\mathbb{R}^N$ spanned by the eigenvectors and generalized eigenvectors of $J(x)$ corresponding to the eigenvalues μ_k, $k = 1, ..., p$. Let $V_p \in \mathbb{R}^{N\times p}$ denote an orthogonal basis of U, i.e., the columns of V_p are orthogonal and span the subspace U. Finally, let $V_q \in \mathbb{R}^{N\times(N-p)}$ be an orthogonal basis of $U^\perp$, the orthogonal complement of U in $\mathbb{R}^N$.

The idea is to decompose the correction Δx into a component in U and a component in $U^\perp$. For this decomposition we construct the orthogonal projectors $P := V_pV_p^T$ onto U, where V_p^T denotes the transpose of the matrix V_p and $Q := V_qV_q^T = I - P$ onto $U^\perp$. Consequently, the correction can be written as

$$\Delta x = P\Delta x + Q\Delta x = V_pV_p^T\Delta x + V_qV_q^T\Delta x = V_p\Delta\bar{p} + V_q\Delta\bar{q}, \tag{23}$$

where the notation $\Delta\bar{p} := V_p^T\Delta x$ and $\Delta\bar{q} := V_q^T\Delta x$ is used.

We would like Δx to be an approximate solution of

$$(J(x) - I)\Delta x = -(F(x) - x). \tag{24}$$

So we substitute (23) in (24) and multiply the left and right hand side of (24) by $(V_p \;\; V_q)^T$. This leads to the matrix equation

$$\begin{pmatrix} V_p^T(J(x)-I)V_p & V_p^TJ(x)V_q \\ 0 & V_q^T(J(x)-I)V_q \end{pmatrix} \begin{pmatrix} \Delta\bar{p} \\ \Delta\bar{q} \end{pmatrix} = -\begin{pmatrix} V_p^T(G_u(x)-x) \\ V_q^T(G_u(x)-x) \end{pmatrix}.$$

Note that the last row of this equation does not contain an expression in $\Delta\bar{p}$. Therefore this row (which contains $N-p$ equations) can be solved for $V_q\Delta\bar{q}$ with the Picard iteration scheme

$$V_q\Delta\bar{q}_{j+1} = V_qV_q^TJ(x)V_q\Delta\bar{q}_j + V_qV_q^T(G_u(x) - x). \tag{25}$$

If the approximation of the solution of (25) is again denoted by $V_q\Delta\bar{q}$, then the equation for $\Delta\bar{p}$ becomes

$$V_p^T J(x) V_q \Delta\bar{q} + V_p^T (J(x) - I) V_p \Delta\bar{p} = -V_p^T (G_u(x) - x).$$

Solving this equation only requires the evaluation of G_u, i.e., one cycle simulation, p times.

Together $V_q\Delta\bar{q}$ and $V_p\Delta\bar{p}$ make up the update in the scheme (22), which, with the decomposition made in (23), can be written as

$$x_{i+1} = x_i + V_p\Delta\bar{p} + V_q\Delta\bar{q}.$$

Because of the way the two subspaces U and $U^\perp$ are constructed, the scheme (25) will converge much faster than the direct substitution method applied to the original system of equations. We refer to (Lust et al., 1998) for more details about the convergence analysis of the method.

The dimension of U is obtained by computing the Jacobian with finite differences and then calculating the eigenvalues and eigenvectors. The eigenvectors and generalized eigenvectors corresponding to the p largest eigenvalues span the subspace U. An orthogonal basis can be obtained using a Gram-Schmidt orthogonalization procedure. Notice that since the Jacobian is available for this first iteration, we can take the first iteration to be a Newton iteration. In the next iterations the basis of the slow subspace is updated with one subspace iteration (Saad, 1992). It is important to note that in this subspace iteration approximations to the p largest eigenvalues of the Jacobian are obtained. These eigenvalues are essential in the determination of the stability of a periodic state.

From the construction of the Newton-Picard method, it can easily be seen that the method is the more efficient as the number of eigenvalues with modulus close to one is smaller.

Now we will look more closely at solutions of the adjoint equations. In the same manner as above, we can define period maps for the adjoint equations (20) and (21). We will concentrate on the equation (20), equation (21) can be treated analogously.

Note that if $A(t)$ solves the initial value problem

$$\begin{aligned} &\frac{d}{dt}A(t) = \frac{\partial F}{\partial x}(t, x(t), u(t))A(t), \\ &A(0) = I. \end{aligned}$$

then $A(1) = J(x(0))$, where $J(x(0)) = \frac{\partial G_u}{\partial x}(x(0))$ denotes the Jacobian of G_u at $x(0)$. This allows us to write the solution to the adjoint equation (20) with initial value $\Lambda(0) = \Lambda_0$ as follows

$$\Lambda^T(t) = \Lambda_0^T A(t)^{-1} - \int_0^t \frac{\partial L}{\partial x}(s, x(s), u(s))A(s)\,ds A(t)^{-1}.$$

Consequently the period map $K : \mathbb{R}^N \to \mathbb{R}^N$ associated with equation (20) is given by

$$
\begin{aligned}
K(\Lambda_0^T) &= \Lambda_0^T A(1)^{-1} - \int_0^1 \frac{\partial L}{\partial x}(s, x(s), u(s))A(s)dsA(1)^{-1} \\
&= \Lambda_0^T J(x(0))^{-1} - \int_0^1 \frac{\partial L}{\partial x}(s, x(s), u(s))A(s)dsJ(x(0))^{-1}.
\end{aligned}
$$

Since the time integration of the adjoint equation is highly unstable forward in time, we can not evaluate this period map, see (Bryson Jr. and Ho, 1975). It is possible, however, to evaluate the inverse of K by integrating equation (20) backward in time. A simple computation shows

$$K^{-1}(\Lambda^T) = \Lambda^T J(x(0)) + \int_0^1 \frac{\partial L}{\partial x}(s, x(s), u(s))A(s)\, ds.$$

Thus, in order to find a periodic solution of (20), it suffices to solve

$$\Lambda^T \big(J(x(0)) - I\big) = -\int_0^1 \frac{\partial L}{\partial x}(s, x(s), u(s))A(s)ds \tag{26}$$

for Λ^T.

Here we see that the inverse period map for the adjoint equations is an affine map with Jacobian equal to the transposed Jacobian $J(x(0))^T$ of the period map G_u corresponding to the state equation at the periodic solution $x(t)$. In what follows, it is shown that this is a useful fact for the application of the Newton-Picard method to the adjoint equations.

Now suppose that the periodic solution $x(t)$ of (15) is computed using the Newton-Picard method. Thus we have $G_u(x(0)) = x(0)$. In the previous section we have seen that the Newton-Picard method is constructed in such a way that it gives approximations to the p largest eigenvalues of the Jacobian $J(x(0))$ of G_u at $x(0)$ and an orthonormal basis V_p of the subspace U that is spanned by the eigenvectors and generalized eigenvectors that correspond to these p largest eigenvalues. In addition we know the Jacobian $J(x(0))$ restricted to the subspace U, which can be written as

$$S := V_p^T J(x(0))V_p.$$

If we multiply both sides of (26) on the right by $(V_p \; V_q)$, we obtain

$$(\Lambda^T V_p \;\; \Lambda^T V_q) \begin{pmatrix} V_p^T J(x(0))V_p - I_p & V_p^T J(x(0))V_q \\ 0 & V_q^T J(x(0))V_q - I_q \end{pmatrix} = (fV_p \; fV_q), \tag{27}$$

where

$$f = -\int_0^1 \frac{\partial L}{\partial x}(s, x(s), u(s))A(s)ds.$$

From equation (27) it follows that with the information from the Newton-Picard solution of the state equation, we can immediately solve for $\Lambda^T V_p = f V_p (S - I)^{-1}$. So if we have found $\Lambda^T V_p$, then we have to solve

$$\Lambda^T V_p (V_p^T J(x(0)) V_q) + \Lambda^T V_q (V_q^T J(x(0)) V_q) - \Lambda^T V_q = f V_q$$

for $\Lambda^T V_q$. This can be done by using the iterative process defined by

$$\lambda_q^{(i+1)} = \lambda_q^{(i)} (V_q^T J(x(0)) V_q) + \Lambda^T V_p (V_p^T J(x(0)) V_q) - f V_q.$$

Note that it is equivalent to iterate

$$(\Lambda^T V_p \;\; \lambda_q^{(i+1)}) = (\Lambda^T V_p \;\; \lambda_q^{(i)}) \begin{pmatrix} V_p^T J(x(0)) V_p & V_p^T J(x(0)) V_q \\ 0 & V_q^T J(x(0)) V_q \end{pmatrix} - (f V_p \;\; f V_q).$$

The Newton-Picard method is constructed in such a way that this last iterative procedure converges with rate equal to the modulus of the $(p+1)$th eigenvalue of $J(x(0))$, which is much faster than the Picard iteration of the inverse of the period map K.

We now would like to make some remarks about the implementation of the Newton-Picard method. Our implementation of the Newton-Picard algorithm performs a fixed number of iterations of the Picard scheme (25). This number is denoted by l in the following description of the steps of the algorithm. The number δ_0 in step 5) is the bound for convergence to a periodic state. In parenthesis, we denote the number of cycle simulations that is needed.

Newton-Picard Algorithm–State Equations

Step 1: *Choose an initial value x_0 and set $i = 0$.*

Step 2: *Compute the Jacobian $J(x_0)$ of G_u at x_0 (finite differences: N+1 cycles).*

Step 3: *Compute the eigenvalues and eigenvectors of $J(x_0)$. This determines p, the dimension of the slow subspace U and an orthonormal basis V_p of U.*

Step 4: $x_1 = x_0 - (J(x_0) - I)^{-1}(G_u(x_0) - x_0)$.

Step 5: *If $|G_u(x_i) - x_i| < \delta_0$ then stop (1 cycle).*

Step 6: *Do s subspace iterations with projection to update V_p ($s \times p$ cycles) and compute $V_p^T(J(x_i) - I)V_p$ (p cycles).*

Step 7: *Do l Picard iterations to compute $V_q \Delta\bar{q}$ (l cycles).*

Step 8: *Compute $\Delta\bar{p}$ (1 cycle). Set $x_{i+1} = x_i + V_p\Delta\bar{p} + V_q\Delta\bar{q}$. Set $i = i+1$. Go to* **Step 5**.

The above algorithm amounts to $p+2+sp+l$ cycles per iteration. In our implementation we take $l=2$ and $s=1$ Thus, for each iteration of the Newton-Picard method, we need $2p+4$ cycle simulations. The main advantage of the method is that, if p is small compared to N, one iteration of the Newton-Picard method will be much more efficient than an iteration of Newton's method.

The implementation of the Newton-Picard method for the adjoint equations can be described with the following four steps

Newton-Picard Algorithm–Adjoint Equations

Step 1: *Choose an initial value* y_0. *Set* $i=0$.

Step 2: *If* $|K^{-1}(y_i)-y_i|<\delta_0$ *then stop (1 cycle).*

Step 3: *Compute* $\tilde{y}=(K^{-1}(y_i)-y_i)V_p(S-I)^{-1}$.

Step 4: *Iterate* l *times:* $\lambda^{(j+1)}=K^{-1}(\lambda^{(j)})$ *with* $\lambda^{(0)}=V_p^T\tilde{y}$ *(l cycles). Put* $y_{i+1}=y_i-\lambda^{(l)}$. *Set* $i=i+1$. *Go to* **Step 2**.

The above algorithm amounts to solving $l+1$ initial value problems for each iteration. In our implementation we take $l=2$. Thus for each iteration of the Newton-Picard method for the adjoint equations we need to solve 3 initial value problems.

4 Conclusions

We introduced an efficient numerical optimization procedure for the computation of solutions to periodic optimal control problems. This procedure consists of a combination of the Newton-Picard method with a first order gradient method. This latter method is able to compute the optimal control of a periodic process under one (or more) nonlocal constraints, such as a minimum product purity constraint. The Newton-Picard method is one of the most efficient methods for the computation of periodic solutions of the state equations (Van Noorden et al., 2002). The method does not only compute periodic solutions to the state equations, but also obtains information about the stability of the computed solution. This information may be used to compute with very little extra computer time periodic solutions to the adjoint equations, needed in the first order gradient algorithm.

Using the presented numerical procedure, we have studied the numerical optimization of two periodic processes: a rapid pressure swing adsorber (Nilchan and Pantelides, 1998) and a rapid pressure swing reactor (Cheng et al., 1998). For both processes we presented the model equations.

First, the two processes were optimized with respect to three time-constant parameters: the cycle duration, the feed pressure, and the ratio between the two steps in the cycle.

Subsequently, we computed for both processes the optimal control of the feed pressure during the pressurization step, using a first order gradient method in combination with the Newton-Picard method. The computed optimal controls improved the performance of the processes considerably, compared to the time-constant parameter optima.

The computed optimal controls suggest that the addition of two more steps in the operating scheme, a pre- and a post-pressurization step in which the feed end of the adsorber or reactor is closed, would also improve the time-constant parameter control performance of the processes. To demonstrate this, we optimized the two processes with respect to five time-constant parameters: the duration of the four steps in the cycle, and the feed pressure during the pressurization step. The found four step cycle optima improved the performance of the optimal two step cycles with approximately 25%. This result extends the result by Kowler and Kadlec (1972), who found that the optimal control of a period adsorber consists of a three step cycle: a pressurization step, a post-pressurization step with no inflow, and a depressurization step.

As a last remark, we would like to point out that the work in this paper shows that the results of a time-dependent parameter optimization can help to gain insight in the solution of a time-constant parameter optimization problem. Also for this reason the optimal control method presented in this paper will prove to be a invaluable tool for the study and design of periodic processes.

5 Notation

5.1 Roman

$c^{(i)}(t,z)$	dimensionless gas phase concentration of component i	-
$q^{(i)}(t,z)$	dimensionless adsorbed amount of component i	-
$v(t,z)$	dimensionless gas phase velocity	-
$r(c^{(1)},c^{(2)},c^{(3)})$	reaction rate	-
$u(t)$	control	-
$x(t)$	solution of state equations	-
F	right-hand-side of state equation	-
G_u	period map	-
J	Jacobian of period map	-
$I(x,u)$	performance index	-
$\tilde{I}(x,u)$	non-local constraint	-
$L(t,x,u)$	defines performance index	-
$M(t,x,u)$	defines non-local constraint	-
$R(t)$	solution to adjoint equation	-
I_j	integrals computed in gradient algorithm, $j=1,2,3$.	-
$k^{(i)}$	isotherm constant	-
$D^{(i)}$	isotherm constant	-
K	reaction equilibrium constant	-

t_1	duration of pre-pressurization step	-
t_2	duration of pressurization step	-
t_3	duration of post-pressurization step	-
t_4	duration of depressurization step	-
T	cycle duration	-
C_1	dimensionless parameter	-
C_2	dimensionless parameter	-
$C_3^{(i)}$	dimensionless parameter ($i = 1, 2, 3$)	-
C_4	dimensionless parameter	-
C_5	dimensionless parameter	-
U	"slow" subspace	-
p	dimension of U	-
V_p	basis of U	-
V_q	basis of $U^\perp$	-
P	projector onto U	-
Q	projector onto $U^\perp$	-
Δx	correction of x	-
K	period map of adjoint equation	-
$y_f^{(i)}$	molar fraction of species i in the feed gas	-
p_w	dimensionless exhaust pressure	-
t_f	ratio between duration of adsorption and desorption step	-
a	constant in definition of compressor power	-
b	constant in definition of compressor power	-
P_0	characteristic power	J/s
V	average power	J/s
Pu	purity of product	-
Y	yield of component B	-

5.2 Greek

$\Lambda(t)$	solution to adjoint equation	-
ϵ_j	damping factors for gradient algorithm, $j = 1, 2$.	-
μ_j	eigenvalue of Jacobian J	-
$[\alpha, \beta]$	control interval	-

5.3 Superscripts

(i)	component i	-

References

Bryson Jr., A. and Ho, Y. (1975). *Applied optimal control.* Washington, D.C., Hemisphere

Publishing Company.

Cheng, Y., Alpay, E., and Kerschenbaum, L. (1998). Simulation and optimisation of a rapid pressure swing reactor. *Comput. Chem. Eng.*, 22:S45–S52.

Horn, F. and Lin, R. (1967). Periodic processes: a variational approach. *Ind. Eng. Chem. Process Design Develop.*, 6:21–30.

Kowler, D. and Kadlec, R. (1972). The optimal control of a periodic adsorber. *AIChE Journal*, 18:1207–1219.

Kvamsdal, H. and Hertzberg, T. (1995). Pressure swing adsorption – optimization of a trace separation system. *Comput. Chem. Eng.*, 19:S339–S344.

Kvamsdal, H. M. and Hertzberg, T. (1997). Optimization of PSA systems - studies on cyclic steady state convergence. *Comput. Chem. Eng.*, 21:819–832.

Lust, K., Roose, D., Spence, A., and Champneys, A. R. (1998). An adaptive Newton-Picard algorithm with subspace iteration for computing periodic solutions. *SIAM Journal on Scientific Computing*, 19:1188–1209.

Nilchan, S. and Pantelides, C. C. (1998). On the optimisation of periodic adsorption processes. *Adsorption*, 4:113–147.

Saad, Y. (1992). *Numerical Methods for Large Eigenvalue Problems*. Algorithms and Architectures for Advanced Scientific Computing, Manchester University Press, Manchester.

Stepanek, F., Kubicek, M., and Marek, M. (1998). Modeling and optimization of continuous adsorption in a dessicant rotor. *Industrial and Engineering Chemistry Research*, 37:1435–1443.

Van Noorden, T. L., Verduyn Lunel, S. M., and Bliek, A. (2001). The efficient computation of periodic states of cyclically operated chemical processes. Technical Report MI 2001-22, Mathematical Institute, University of Leiden.

Van Noorden, T. L., Verduyn Lunel, S. M., and Bliek, A. (2002). Acceleration of the determination of periodic states of cyclically operated reactors and separators. *accepted for publication in Chemical Engineering Science.*